ISSN: 2716-9227 Algerian Journal of Engineering and Technology 08 (2023) 277–287 e-ISSN: 2716-9278

Algerian Journal of Engineering and Technology

Journal homepage: https://jetjournal.org/index.php/ajet

Original Article

Effects of desilication and dealumination of NaA zeolite on uranium recovery from aqueous effluents

Faiza Oudjer [a]*, Sihem Khemaissia [a], Leila Mouhelbi [a], Sihem Outtas [a], Yasmina Hammache [a], Yasmine Meddour [b], Habiba Chouial [b]

[a] *Draria Nuclear Research Centre, P.43 16050, Sebala, Draria, Algiers,Algeria*
[b] *University of Science and Technology Houari Boumediene, Algiers, Algeria*

ARTICLE INFO

Article history:
Received 08 October 2023
Revised 10 Novembre 2023
Accepted 13 Novembre 2023

Keywords:

NaA ;
Uranium ;
Adsorption;
Desilication;
Dealumination.

ABSTRACT

Different processes for recovering uranium from raffinates and effluents generated throughout the nuclear fuel cycle are implemented. The adsorption process has been widely adopted in the uranium recovery from aqueous solution, due to its simplicity, rapid kinetics, wide applicability, cost-effectiveness and non-secondary contamination. Adsorption performance is directly determined by the appropriate adsorbents for the target compounds. Zeolite is one of the most commonly used materials for adsorption due to its low cost, high chemical and thermal stability. However, its relatively low sorption capacity limits its performance and feasibility. Many modification strategies have been used to improve its performance. Desilication and dealumination are among the processes that improve accessibility to active sites located inside the zeolite framework and can limit diffusion constraints through the creation of a secondary network of large pores (mesopores) connected to native micropores. In this study, the synthesized and modified NaA zeolite were characterized by powder X-ray diffraction (XRD), thermogravimetric analysis (TGA), Fourier transform infrared spectroscopy (FTIR) and nitrogen adsorption-desorption analysis. Uranium adsorption capacities were found to be around 42 mg/g, 27 mg/g and 10 mg/g for desilicated NaA, NaA and dealuminated NaA respectively. The desilicated NaA material showed better selectivity compared to the starting material. The adsorption of UO_2^{2+} ions follows the Langmuir isotherm and the pseudo-second-order kinetic model. The values of uranium desorption 36%, 82% et 87% for NaA, desilicated NaA and dealuminated NaA have been reached using 1M HNO_3 for one treatment cycle. The treatment of the real effluent with the three adsorbents showed a recovery of around 62% in uranium for NaA and desilicated NaA, for dealuminated NaA it was around 19% following the coadsorption of competing metal ions.

1. Introduction

During the operation of nuclear installations, from the extraction or processing of uranium to the production of uranium dioxide, significant quantities of aqueous effluents are generated, which represent a significant nuisance due to the presence of transuranic elements, hence the separation and/or recovery of uranyl ions is essential. Several investigations have been carried out for the effective removal or recovery of uranium, a wide range of different treatment processes like precipitation, co-precipitation [1], electrodeposition [2], electrocoagulation [3], microbiological methods [4], solvent extraction [5], ion exchange [6], membrane filtration [7] and adsorption [8-10] have been developed. Adsorption has proven to be a very effective and widely used method in industry and ranks second after precipitation in terms of frequency of use or study. Among microporous solids, we find porous

* *Corresponding author*
E-mail address: f-oudjer@crnd.dz, s-khemaissia@crnd.dz
Peer review under responsibility of University of El Oued.
 https://dx.doi.org/10.57056/ajet.v8i2.134

and crystalline zeolites; they are used in many separation processes thanks to their physicochemical properties. Their porous structure generates a large specific surface area, which gives them different properties such as high cation exchange capacities, adsorption efficiency and resistance to radiation [11]. Zeolites make it possible to efficiently extract radionuclides and other toxic metals such as iron, cadmium, copper, chromium, and lead from effluents [12]. Despite the application of zeolites in different fields, in certain cases, their use still encounters problems of diffusion of the molecules adsorbed in the microporous network. The latter is linked to the shape, size and connectivity of the intra-framework channels. This internal characteristic of certain zeolites generates confinement effects, which themselves can impose severe constraints such as the difficulty of accessing active sites. This is why a large research effort has been developed in the field of porous materials to find materials with interesting properties in the adsorption of bulky molecules. For this purpose, a booming field such as new hierarchical microporous solids is beginning to provide effective and original solutions to these diffusion problems. Several processes used have led to obtaining hierarchical zeolites and have opened new perspectives by showing improved performance compared to untreated ones. The framework of zeolites is likely to be modified either during synthesis or after synthesis (post-synthesis) [13]. The thermal or chemical treatment of a zeolite inevitably leads to a modification of its Si/Al ratio. Various approaches have been proposed, either the direct development of mesoporous materials or the development of mesoporous zeolites using several processes such as dealumination [14], desilication [15], organic complex (template) [16, 17], use of polymers, solid matrices, etc. to generate additional porosity and remedy the problem of restricted pore openings in zeolitic crystals.

In our work, we will see the effect of combining dealumination and desilication treatments on the structure of the NaA zeolite prepared from gel composed of a source of silicon and aluminium and elaborated by hydrothermal synthesis. Hierarchical zeolites will be obtained using alkaline and acidic treatments to prevent dealumination and desilication and will be evaluated for the ability to remove the hexavalent uranium from aqueous solutions under various conditions such as pH, contact time, S/L ratio and different uranium concentrations and to determine the optimum procedure. Adsorption isotherms have been analysed by Langmuir, Freundlich and Dubinin-Radushkevich models. The kinetics of recovery was also studied. In conclusion, we highlight the performances of different materials in uranyl ions adsorption from effluents generated during the processing uranium ore.

2. Materials and Methods

2.1. Synthesis of the adsorbent

The LTA zeolite was synthesized hydrothermally from a gel with the following molar composition: $1.1Na_2O$ 1.26 SiO_2 Al_2O_3 $92H_2O$, the gel was brought in a stainless steel autoclave to a temperature of 90°C in an oven for 72 hours. At the end of the synthesis, the product is filtered, washed with distilled water and dried at 105°C in an oven. [18]. Desilicated zeolite NaA was prepared by alkaline treatment of zeolite NaA, using NaOH solution [19] at a concentration of 1 M as a desilication agent and a ratio (Liquid/Solid) of 10 mL/g. The dealuminated NaA zeolite was prepared by acid treatment of the NaA zeolite, using the HCl solution [20] at a concentration of 0.1 M as a dealuminating agent and a ratio (Liquid/Solid) of 10 mL/g, before the dealumination we must obtain the ammoniacal form of the zeolite then the protonated form. Obtaining the ammoniacal form of the NaA zeolite consists of heating, under reflux, the NaA material in a 0.1 M ammonium nitrate solution with a ratio RS/L=50 g/L. The zeolite is filtered and washed with distilled water up to pH=7, dried in an oven at 60°C and finally calcined for 4 hours at 550°C to obtain the protonated form (H-NaA).

2.2. Characterization

The synthesized material is analyzed by a BRUKER AXS D8 Advance type X-ray diffractometer with Cu-Kα (λ= 1.5406 Å) in the range of 5-60°. The infrared spectra were recorded over a range of 400-4000 cm^{-1} by a PERKIN ELMER UATR Two spectrometer. The thermal analysis of the sample was carried out on a LABSYS thermoanalyzer of SETARAM TGA/TDA type in the temperature range from 298 to 1073K with a heating rate of 10°C/min. The surface area measurement was conducted by the BET method, pore size distribution and pore volume with the BJH model using MICROMERITICS ASAP 2010 device.

2.3. Reagents

1 g/L stock uranium solution (from the uranium purification laboratories of the Draria Nuclear Research Center, declared in the framework of IAEA guarantees) was prepared by dissolving a quantity of uranyl nitrate salt UO_2 $(NO_3)_2 6H_2O$ (Merck, 99% purity) in distilled water. Uranium solutions from 10 mg/L to 300 mg/L were prepared from the 1 g/L stock solution by appropriate dilutions. The pH is adjusted with nitric acid HNO_3 and sodium hydroxide NaOH.

2.4. Instrumentation

The uranium (VI) concentrations are determined by a UV-visible spectrophotometer (Cintra 40 with GBC software). The adsorption experiments were carried out using the batch protocol using an HS 500 Jankel & Kunkel Ika-Werk model shaker. The Hanna Instrument model 2210 pH meter is used for pH reading. A Heraeus Labofuge 601 model centrifuge is used to separate the liquid from the material. A Prolabo oven is used to dry the produced solid. Flame atomic absorption spectroscopy is used to determine the concentrations of impurities in the effluent.

2.5. Adsorption experiments

The different experiments are carried out in closed ployethylene bottles of 100 mL capacity, where we introduce 0.1 g of the different materials with 10 mL of uranium ion solution of know concentration. The mixture is stirred using a shaker at room temperature. The two phases are separated by centrifugation. The filtrates obtained were analyzed spectrophotometrically using Arsenazo III method [21, 22] at 652 nm. The calculation of the uranium adsorption efficiency is given by the following formula:

$$\%d'adsorption = \left[\frac{C_0 - C_f}{C_0}\right] \times 100 \quad (1$$

$C_{0:}$ Initial concentration of uranium (mg/L),
$C_{f:}$ Final concentration of uranium (mg/L),
The adsorption capacity Qe is calculated from the following equation:

$$Q_e = \left(C_0 - C_e\right)\left[\frac{V}{m}\right] \quad (2$$

C_e: Concentration of uranium at equilibrium (mg/L),
V: Volume of solution (L),
m: Mass of the adsorbent (g).
The optimization tests were carried out for an initial uranium concentration of 100 mg/L. For the isothermal study, the uranium concentration varied from 10 to 300 mg/L; the experiments were carried out at room temperature.

3. Results and Discussion

3.1. Characterization of the adsorbents elaborated

The purity of the materials elaborated NaA, desilicated NaA and dealuminated NaA is verified by X-ray diffraction. The diffractograms are compared to that of structural type NaA. The diffractogram is typical of a Linde A crystal structure Fig.1.Dealumination and desilication treatments of Linde zeolite result in significant changes in the intensity, width and position of the XRD peaks, but no structural collapse or peak broadening or baseline separation was observed, which would be characteristic of the presence of an amorphous phase [23]. The result of the FTIR analysis is illustrated in Fig.2., this analysis was carried out to identify the formation of the NaA framework. It shows that the treatment did not modify the zeolite framework. Desilcated and dealuminated zeolites exhibited typical Linde A. The characteristic bands at 1400-400 cm^{-1} are attributed to zeolite structure. The band at 464 cm^{-1} and 462 cm^{-1} relates to the bending vibration of tetrahedral T-O, like AlO_4 and SiO_4 in the zeolite [24]. The bands at 579 and 574 cm^{-1} are assigned to the external vibration of double four-rings [25]. The signal at 720 cm^{-1} is due to the symmetric stretching vibration Al-O. The bands at 771cm^{-1}, 776 and 788 cm^{-1} are attributed to symmetric elongation of Si-O-Al and Si-O-Si. The bands at 1008, 1032 and 1021 cm^{-1} were assigned for the internal vibration of (Si, Al)-O asymmetric stretching. The band located around 1643 cm^{-1}, 1639 cm^{-1} and 1638 cm^{-1} were attributed to the bending of –OH groups due to the possible adsorption of moisture [26]. The band at ~3460 cm^{-1} is also related to asymmetric stretching of –OH because of physically adsorbed water or surface hydroxyl groups. This band is wider in the desilicated sample than the parent NaA due to the higher surface area caused by the treatment process. It can be seen that the FTIR spectra are in agreement with XRD patterns and confirm the presence of NaA structure even with the treatment process on the desilicated and dealuminated samples.
The thermogravimetric curve for NaA, NaA desilicated and NaA dealuminated, shown in Fig.3. indicates a total mass loss of the order of 18.7%, 27.88% and 16% respectively between 50 and 1000 C°, which corresponds to dehydration or elimination of physisorbed water between 50 and 200°C. The water mass loss increases with the decrease in the SiO_2/Al_2O_3 ratio, this result is in agreement with the literature, the hydrophobicity increases with the increase in the Si/Al ratio [27, 28]. This result means that desilication has taken place. The desilication treatment was accompanied by significant weight loss; the same result was found [29]. Nitrogen adsorption made it possible to evaluate the specific surface areas of NaA, desilicated NaA and dealuminated NaA materials. For the NaA material, the specific surface area value is 771.63 m^2/g, for desilicated NaA the specific surface area value is 888.42 m^2/g and for dealuminated NaA the specific surface area value is 330.62 m^2/g.

Table 1: Data obtained from adsorption isotherms

Adsorbent	Specific surface area BET (m^2/g)	Microporous volume (cm^3/g)
NaA	771.63	**0.26**
Desilicated NaA	888.42	**0.32**
Dealuminated NaA	**330.62**	**0.11**

We note that the desilication process was able to slightly increase the specific surface area following the departure of silicon from the crystal structure and the process therefore created sorption sites due to the enlargement of the surface area [30]. On the other hand, the process of deamination reduced the specific surface area of the NaA material. The textural properties of the NaA zeolite were not modified; there was no significant difference in the surface area which went from 771 m^2/g to 888 m^2/g, this slight increase observed in the SBET after desilication is also reported in the literature [31].

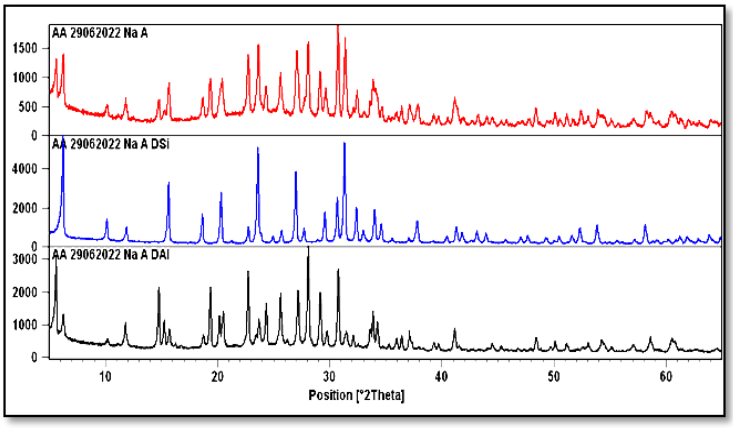

Fig 1. XRD patterns of the NaA zeolites

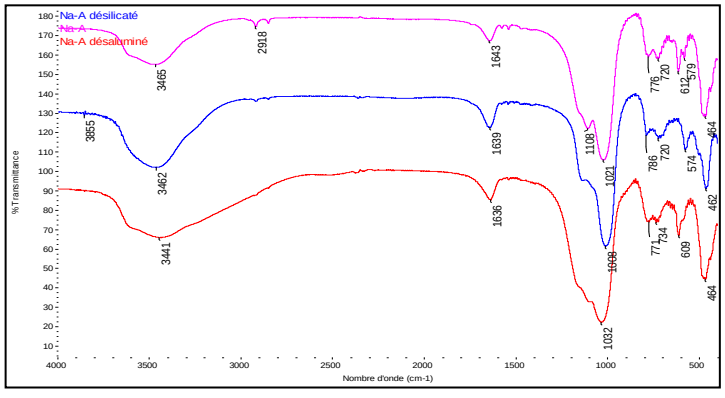

Fig 2. FTIR of the NaA zeolite by different treatments.

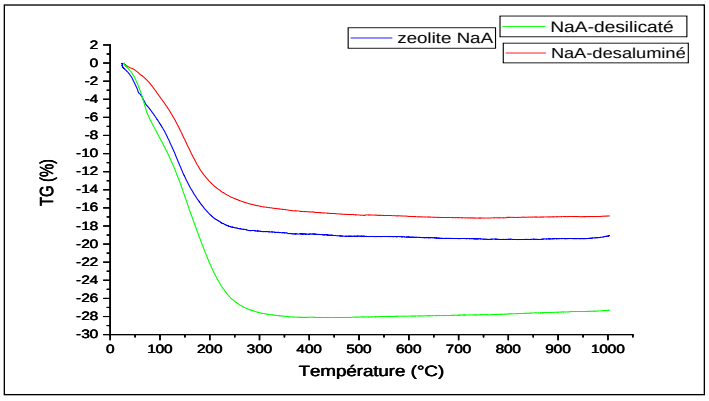

Fig 3. GTA curves of NaA zeolite A

3.2. Effect of pH on the adsorption of uranyl ions

The effect of pH on the adsorption of uranyl ions was studied in the range from 1.5 to 9.0. The results of the experiments are illustrated in Fig 4. The recovery rate of uranium by the three adsorbents is much greater at acidic pHs. The adsorption percentage is at a maximum at pH 2.5 where the adsorption percentage is 96.36% for the NaA zeolite and 96.88% for the desilicated NaA. For the dealuminated NaA, the maximum adsorption is at pH 6 with a percentage of around 64.77%, this is due to the hydrolysis of the uranyl ion and its release, the uranyl ions UO_2^{+2} in this pH zone between 1 and 4 are free and available, which means that adsorption is favoured, there is no precipitation of uranium in these zones. Even at low pH, there is competition between H^+ ions and the UO_2^{2+} ion for active sites [32]. The formation of bonds between the uranyl ion and the material results in the displacement of the sodium ion from the active sites by the latter, with a further increase of the pH value, the sorption capacity decreases. The formation of stable complexes uranium species $[UO_2(OH)^+, (UO)_3(OH)_5^+, (UO_2)_2(OH)_2]^{2+}$,… etc) [33, 34] could be the main reason for the subversion of the adsorbent [35].

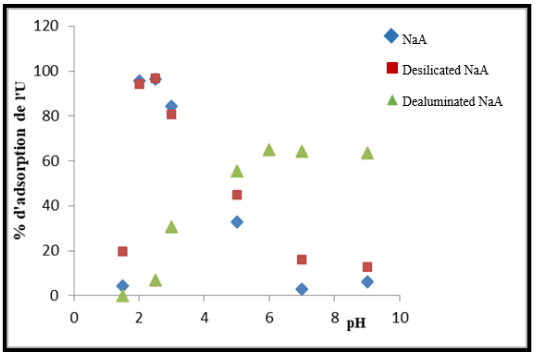

Fig 4. Effect of pH on the adsorption of uranyl ions by the materials elaborated.

3.3. Effect of contact time on uranium recovery

The effect of contact time on the adsorption of uranyl ions on the three materials was studied over a time interval ranging from 2 to 360 min Fig 5. The adsorption efficiency of uranyl ions on NaA, desilicated NaA and dealuminated NaA materials increases with time until a plateau is obtained. The maximum adsorption efficiency is obtained for a contact time of 2 hours for the three materials. The kinetics of the recovery of U(VI) consisted of two phases: an initial rapid phase where sorption was fast and a lower second phase. Initially, all active sites on the adsorbent surface are vacant and the solution concentration is high. After that period, few active sites on the adsorbent are available, so only a very small increase in the sorption is observed. A contact time of 2 hours is retained as the time necessary to reach equilibrium.

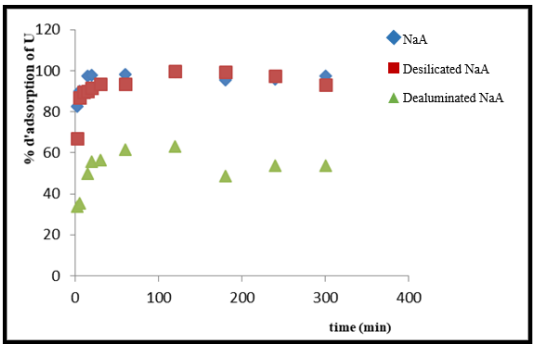

Fig 5. Effect of contact time on the adsorption of uranyl ions on the materials elaborated.

3.4. Effect of the solid/liquid ratio on the adsorption of uranyl ions

The adsorbent dose is an important parameter because it can determine the capacity of an adsorbent for a given initial metal ion concentration. The effect of the ratio (solid/liquid) on the adsorption of uranium (VI) was studied using different ratios (3, 5, 7, 10 and 15 g/L). The results are presented in Fig 6. The adsorption capacity of uranyl ions increases with the increasing mass of the adsorbent, which implies an increase in the number of binding sites available for the adsorption of metal ions. Maximum elimination of U (VI) ions has been achieved, and the maximum adsorption of uranium by the materials is reached for a solid/liquid ratio of 7g/L, with an adsorption percentage of 94.43% for the NaA zeolite. and 93.43% for desilicated NaA, and dealuminated NaA the maximum is reached for a ratio of 10 g/L with an adsorption percentage of the order of 63.10%. Beyond this ratio, we notice a decrease in the quantity adsorbed, this is due to the saturation of the active sites during the adsorption process [36].

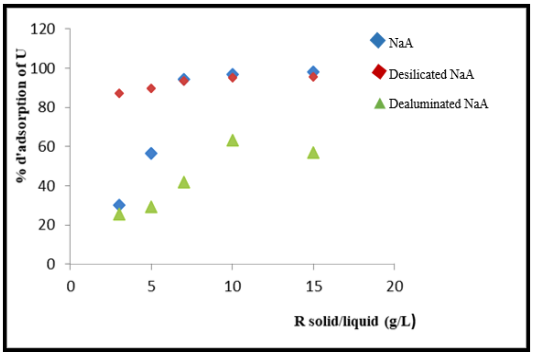

Fig 6. Effect of the solid/liquid ratio on the adsorption of uranyl ions by the materials elaborated.

3.5. Effect of concentration on the adsorption of uranyl ions

The effect of varying the initial concentration of uranium on its adsorption by the three materials was studied in the concentration range of 10 to 300 mg/L Fig 7. The percentage of adsorption of the uranyl ion on the three adsorbents decreases with the increase in the concentration of uranium, this is due to the high mobility of the UO_2^{2+} ion in diluted solutions and therefore to its greater interaction with the adsorbent. The adsorption efficiency tends to decrease when the initial concentration of uranyl ions increases [37]. At lower concentrations, all uranium molecules present in the medium can interact with the adsorption sites located on the surface of the adsorbent, hence higher adsorption efficiencies were obtained. On the other hand, at higher concentrations, lower adsorption yields were observed due to saturation of the adsorption sites [38].

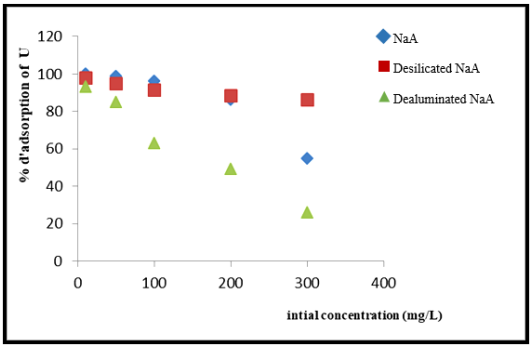

Fig 7. Effect of the initial concentration of uranium on the adsorption of uranyl ions by the materials elaborated.

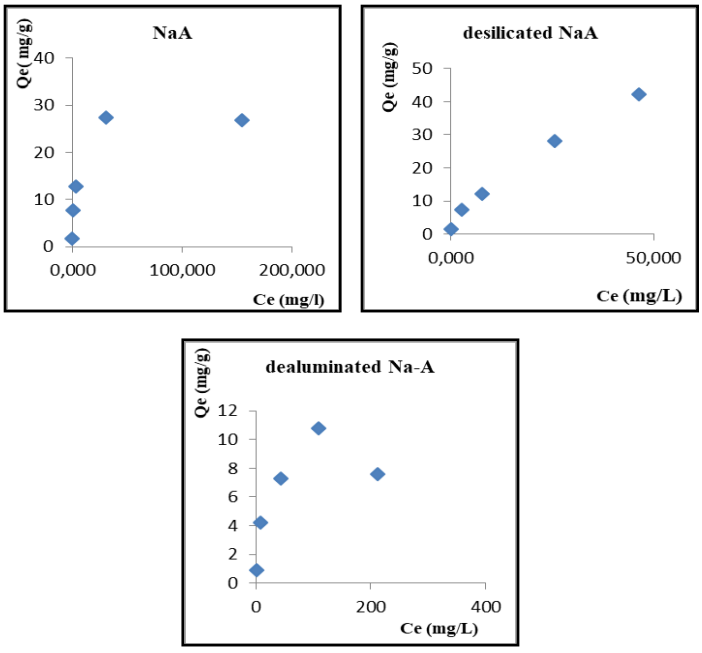

Fig 8. Effect of equilibrium uranium concentration on sorption capacity onto NaA, desilcated-NaA and dealuminated-NaA materials.

The adsorption capacity increases with the increase in the concentration of uranium until reaching the maximum of 10 mg/g for dealuminated NaA with an S/L ratio of 10 g/L, beyond this ratio the adsorption capacity will decrease. NaA reaches the maximum of 27 mg/g with a ratio of 7g/L and the formation of a plateau corresponds to the saturation of the adsorbent. A maximum value of 42 mg/g for the desilicated NaA material was obtained in the concentration range of 10-300 mg/L, the variation of the capacity is linear, and the latter shows that the number of free sites remains constant during adsorption, this means that the sites are created during adsorption by solute molecules which have modified the substrate texture by opening pores.

3.6. Modeling of adsorption isotherms

The sorption isotherm reveals the nature of the adsorption which is directly linked to the surface properties of the adsorbent materials and their affinity with the adsorbate. It also gives an idea about the adsorbate ions distribution on the solid–liquid interface at equilibrium. Langmuir, Freundlich and Dubinin-Radushkevich (R-D) models were tested for the simulation of the uranium adsorption isotherm data.

3.6.1. Langmuir isotherm

The Langmuir model [39] is based on the hypothesis which says that the maximum adsorption capacity corresponds to complete coverage of a monolayer of molecules on the surface of the adsorbent, without interaction between the adsorbed molecules. The Langmuir equation for a homogeneous surface is presented by the following relation:

$$\frac{C_e}{Q_e} = \frac{1}{KQ_{\max}} + \frac{C_e}{Q_{\max}} \quad (3$$

Qe: Quantity of solute adsorbed per unit mass of the adsorbent at equilibrium (mg/g),
K: Langmuir constant (L/mg),
Qmax: Maximum quantity adsorbed per unit of mass (mg/g),
Ce: Concentration of the solute in the liquid phase at equilibrium (mg/L).
Figure 9 presents the adsorption isotherm of uranium on the zeolites NaA, desilicated NaA and dealuminated NaA at room temperature. The Langmuir constants, Qmax and K can be obtained from the slope and the linear intercept.

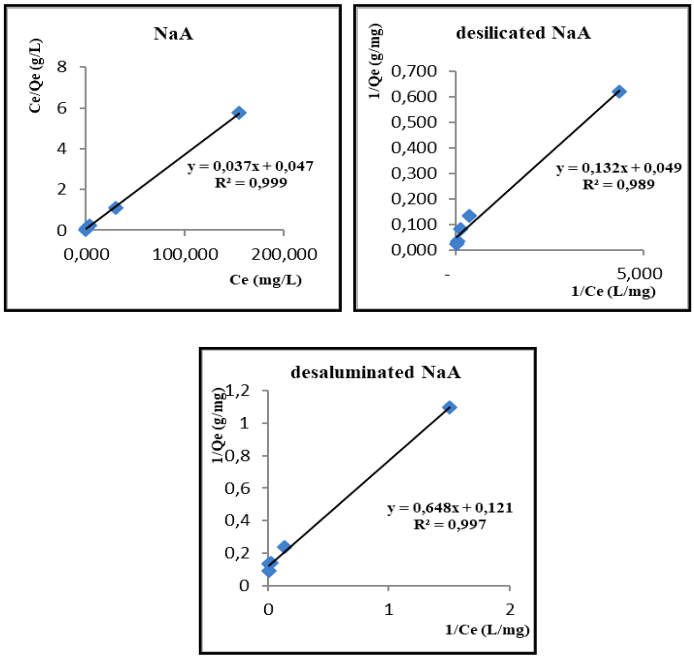

Fig 9. Isotherm of adsorption of uranyl ions on NaA, desilicated NaA and NaA dealuminated according to the Langmuir model.

3.6.2. Freundlich isotherm

The Freundlich isotherm [40] is a model which represents adsorption on heterogeneous multilayer surfaces. The linear form of the Freundlich equation is given by the following equation:

$$LogQ_e = LogK_F + \frac{1}{n}.LogC_e \quad (4$$

K_F (mg/g): Freundlich constant associated with adsorption capacity,

1/n: Freundlich constant associated with adsorption intensity.

Figure 10 presents the adsorption isotherm of uranium on the zeolites NaA, desilicated Na and dealuminated NaA at room temperature according to the Freundlich model.

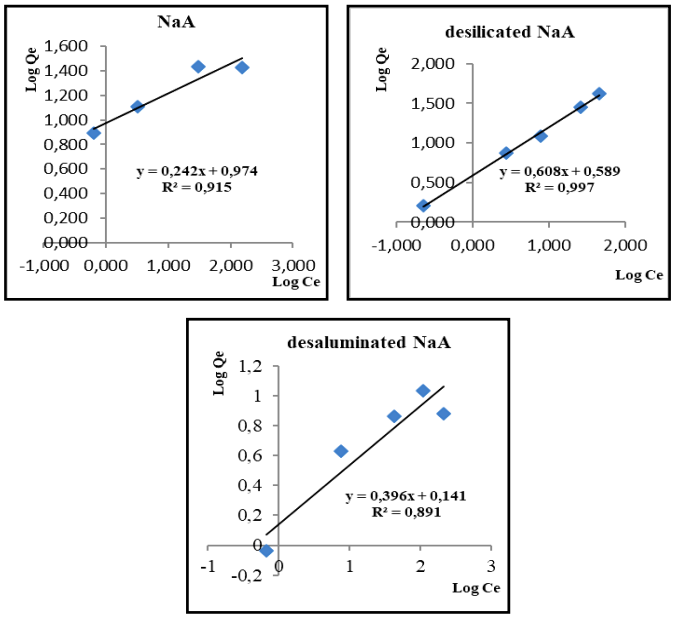

Fig 10. Isotherm of adsorption of uranyl ions on NaA, desilicated NaA and NaA dealuminated according to the Freundlich model.

3.6.3. Dubinin-Radushkevich isotherm (D-R)

The Dubinin-Radushkevich (D-R) isotherm [41] assumes that the surface of the material is heterogeneous. This model is more general than the Langmuir and Freundlich isotherm, it can be used to describe adsorption on both types of homogeneous and heterogeneous surfaces. The linear form of the equation of (D-R) is given by the following equation:

$$LnQ_e = LnQ_m - K\varepsilon^2 \quad (5$$

K (KJ^2/mol^2): Adsorption energy constant,

Qm: Adsorption capacity,

Ɛ the Polanyi potential is given as follows:

$$\varepsilon = RTLn\left(1+\frac{1}{Ce}\right) \quad (6$$

R: Ideal gas constant (8.314 J/mol.K),

T : Temperature in Kelvin (K).

The values of Qm and K are deduced from the graph Ln Qe=f ($Ɛ^2$), and the adsorption energy Ea is calculated from the equation:

$$Ea = \frac{1}{(2K)^{1/2}} \quad (7)$$

If 1<Ea (KJ/mol)<8, the dominant mechanism is physisorption. If 8< Ea (KJ/mol) < 16, chemisorption wins [42].

Fig.11. presents the adsorption isotherm of uranium on the zeolites NaA, desilicated-Na and dealuminated-NaA at room temperature according to the Dubinin-Radushkevich (D-R) model.

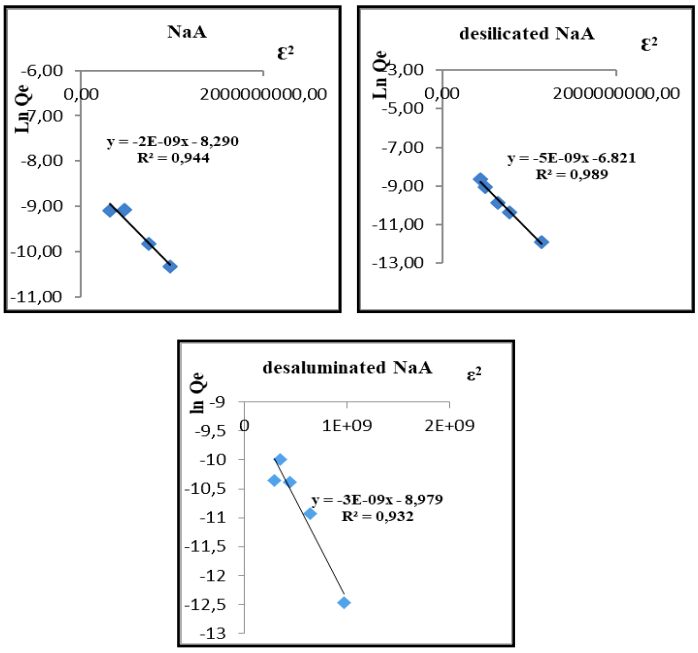

Fig 11. Isotherm of adsorption of uranyl ions on NaA, desilicated NaA and NaA dealuminated according to the Dubinin-Radushkevich (D-R) model.

The isotherm constants, as well as the values of the correlation coefficients of the Langmuir, Freundlich and Dubinin-Radushkeviche (D-R) isotherms, are mentioned in Table (2,3 and4).

Table 2: Constant of the isotherms of *Freundlich model* and the R^2 values of the adsorption of Uranyl ions on the materials NaA, desilicated NaA and dealuminated NaA

Adsorbent	**Freundlich model**		
	K_f (mg/g)	**n**	**R^2**
NaA	9.42	4.13	0.92
Desilicated NaA	3.88	1.65	0.99
Dealuminated NaA	1.38	2.53	0.90

Table 3: Constant of the isotherms of *Langmuir model and* the R^2 values of the adsorption of Uranyl ions on the materials NaA, desilicated NaA and dealuminated NaA

Adsorbent	*Langmuir model*		
	Q_{max} (mg/g)	K_L (L/mg)	R^2
NaA	27.03	0.79	**0.999**
Desilicated NaA	20.40	0.38	**0.990**
Dealuminated NaA	8.26	0.19	**0.997**

Table 4: Constant of the isotherms of *D-R-model* and the R^2 values of the adsorption of Uranyl ions on the materials NaA, desilicated NaA and dealuminated NaA

Adsorbent	*D-R-model*			
	Qm (mol/g)	K_{D-R} (mol/L)	Ea (KJ/mol)	R^2
NaA	$1.24.10^{-4}$	2.10^{-9}	**15.81**	0.950
Desilicated NaA	$1.09.10^{-3}$	5.10^{-9}	**10**	0.989
Dealuminated NaA	$1.26.10^{-4}$	3.10^{-9}	**12.91**	0.930

From the values of the correlation coefficients of the Freundlich, Langmuir and Dubinin-Radushkevich (D-R) models given in Table 1, it follows that the Langmuir isotherm model turned out to be suitable for describing single-component sorption of uranyl ions by the zeolite NaA, desilicated NaA and dealuminated NaA, the maximum sorption responds to the saturation of a monolayer of ions on the surface of the sorbent, and there is no transmigration from the adsorbate to the surface of the zeolite, the model is based on the chemical interaction between the sorbent particles and assumes a constant number of free active sites [37]. The type of adsorption of uranyl ions on NaA, desilicated NaA and dealuminated NaA materials is chemical because the value of Ea is greater than 8 KJ/mole [43].

3.7. Adsorption kinetics

Two kinetic models were used to examine the reaction mechanism (pseudo-first order, and pseudo-second order) [44, 45].

The equations related to the pseudo-first order and pseudo-second order kinetic models are given as follows:

Pseudo –first-order model:

$$Log(Q_e - Q_t) = LogQ_e - \frac{K_{1ads}}{2.303}.t \qquad (8$$

Pseudo-second-order model:

$$\frac{t}{Q_t} = \frac{1}{h} + \frac{1}{Q_e}.t \qquad (9$$

k_{1ads} (min^{-1}): Constant of the pseudo-first order,

K_{2ads} (g/mg. min): Constant of the pseudo-second order,

Qe: Quantitie of uranium (VI) adsorbed in (mg/g) at equilibrium,

Qt: Quantitie of uranium (VI) adsorbed in (mg/g) at time t.

The values of Qe, k_{1ads} and k_{2ads} were determined from the graphs shown in Figures 12 and 13.

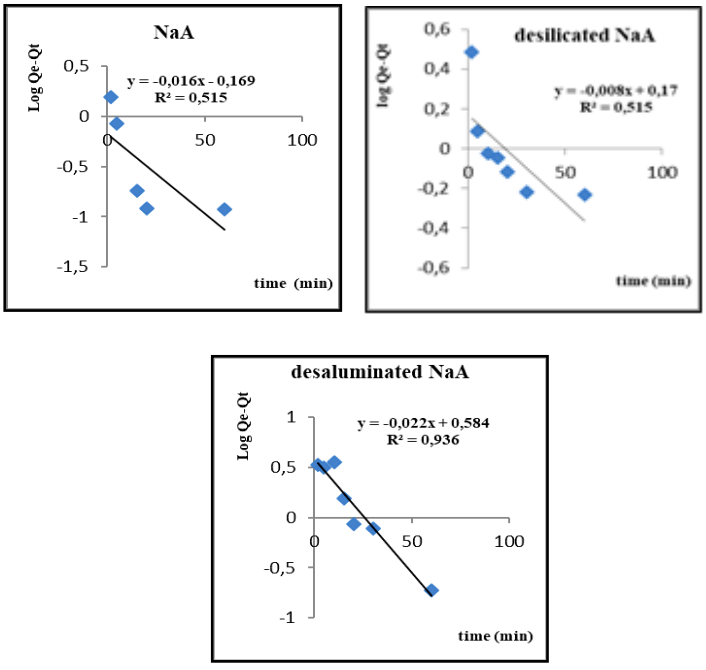

Fig 12. Pseudo-first order kinetic model of uranium adsorption on NaA, desilicated NaA and desaluminated NaA materials

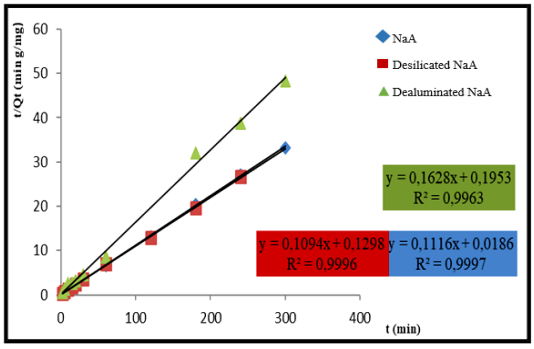

Fig 13. Pseudo-second order kinetic model of uranium adsorption on NaA, desilicated NaA and dealuminated NaA materials.

The kinetic parameters of the models, first and second orders of the adsorption of uranium on NaA, desilicated NaA and dealuminated NaA materials are illustrated in Table 5.

Table 5: Pseudo-first order and pseudo-second order constants for NaA, desilicated NaA and desaluminated NaA materials.

Adsorbents	Pseudo –first-order			Pseudo-second-order			
	Qe mg/g	K_{1ad} min^{-1}	R^2	Qe mg /g	K_{2ads} g/mg min	h mg/ g min	R^2
NaA	0.845	0.0368	0.515	9.009	0.684	55.55	**0.999**
Desilicated NaA	1.185	0.0184	0.515	9.174	0.092	7.752	**0.999**
Dealuminated NaA	1.793	0.051	0.936	6.173	0.135	5.128	**0.996**

According to the results in Tables (2,3and4), the adsorption of uranyl ions is correctly described by the pseudo-second-order kinetic model, with $R^2 > 0.99$. According to Ho and McKay [43], the adsorption is of the chemisorption type, with the formation of valence bonds between the surface functions of the NaA zeolite material and the uranyl ions. It is more likely to be predicted that during the adsorption process, valence forces are formed through the sharing of electrons between the uranyl ions and the adsorbent [46].

3.8. *Desorption and regeneration*

To estimate the reversibility of uranium sorption, desorption experiments using different concentrations of nitric acid (0.01; 0.05; 0.1; 0.2; 0.5 and 1N) with a ratio solid/liquid of 7g/L for NaA and desilicated NaA and 10g/L for dealuminated NaA were carried out at room temperature. The results are presented in Figure 14.

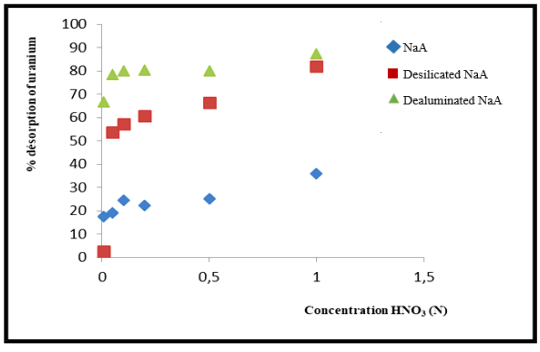

Fig 14. Effect of nitric acid concentration on desorption efficiency uranium on NaA, desilicated NaA and desaluminated NaA materials.

The desorption percentage increases with increasing nitric acid concentration for all three materials, this nitric acid concentration is sufficient for the desorption process for the desilicated NaA and dealuminated NaA materials and possible for the NaA material, it is necessary to increase the concentration of nitric acid under these conditions.

For the NaA material the maximum desorption does not exceed 36%, but for the desilicated NaA and dealuminated NaA materials, the percentages reach almost 82% and 87% respectively for one treatment cycle.

3.9. *Application of the materials developed NaA, desilicated NaA and dealuminated NaA in the treatment of real uranium effluent*

This part concerns the application of the materials, NaA, NaA desilicated and dealuminated NaA in the treatment of uranium effluents from an ore processing operation. These effluents are diverse and contain significant quantities of uranium and toxic metals whose concentrations are variable and often exceed the required standards (Table 4). Treatment by adsorption on the materials NaA, desilicated NaA and dealuminated NaA using the conditions optimal adsorption conditions determined in this work on synthetic uranium solutions. The analysis results are presented in Table 5.

Table6: The concentrations of elements in a real uranium effluent

Element	Uranium	Fe	Mg	Cu	Zn	Mn	Ni	Cd
Concentration (mg/L)	**114.91**	4.594	2.033	0.331	1.5	0.210	0.001	-

Table 7: The percentage of adsorption of uranium on the different materials elaborated

Material	NaA	Desilicated NaA	Dealuminated NaA
% adsorption of uranium	62.41	63.68	19.10

The best adsorption efficiency is achieved with NaA and desilicated NaA materials; the use of these materials in the recovery of uranyl ions is essential.

4. Conclusion

The development of a material with hierarchical porosity with a large specific surface area, capable of recovering uranyl ions as much as possible from aqueous effluents was our objective. We demonstrated that the dealumination of zeolite NaA with acid revealed changes in the hydrophilic behavior of modified zeolite and the desilication process was able to slightly increase the specific surface area following the departure of silicon from the crystal structure and the process therefore creating sorption sites due to the enlargement of the surface area. The recovery process depends on several agents such as initial pH, contact time S/L ratio, and initial uranium concentrations. The experimental data for U (VI) is consistent with the pseudo-second-order kinetic model

of the recovery isotherm models tested, the Langmuir one gave the best fit to the experimental data for U (VI), revealing that the uptake of U(VI) ions can occur via the chemical mechanism and formation of a monomolecular layer. It was found that the recovery capacity is 10 mg/g, 27 mg/g and 42 mg/g for dealuminated NaA, NaA and desilicated NaA respectively.

Furthermore, the adsorbents after the removal of uranium could be regenerated for repeated use using 1M HNO_3. The optimized parameters have been applied to the uranium effluents. It has been found that the uranium (VI) recovery yields are 62 %, 63% and 19% for NaA, desilicated NaA and dealuminated NaA respectively.

The results allow us to state, that the desilication might be a promising sorbent suitable for uranium (VI) recovery from aqueous solutions.

Conflict of Interest: The authors declare that they have no conflict of interest

References

1. Kornilov A, Piterkina E, Shcherbakova K, Makarov, Dmitrieva O. Specific features of peroxides precipitation of uranium from water-ethanol solutions. *Radiochemistry*.2020; 62:173-176
2. Bing-qing Lu, Mi Li, Xiao-wen Zhang, Chun-mei Huang, Xiao-yan Wu, Qi Fang. Immobilization of uranium into magnetite from aqueous solution by electrodepositing approach. *Journal of Hazardous Materials.*2018; 343: 255–265.
3. Shahedi A, Darban A K, Taghipour F, Jamshidi-Zanjan A. A review of industrial wastewater treatment via electrocoagulation processes. *Current Opinion in Electrochemistry*.2020*;* 22: 154–169.
4. Zheng XY, Shen YH, Wang XY, Wang TS. Effect of pH on uranium(VI) biosorption and biomineralization by Saccharomyces cerevisiae. *Chemosphere.* 2018; 203:109-116.
5. Chengtao Yue, Renjuan Liu, Yinghao Yu, Qiyue Wan, Hai Wang, Longcheng Liu, Xu Zhang. Synthesis of novel phosphate-based hyper crosslinked polymers for efficient uranium extraction from radioactive wastewater. *Journal of Water Process Engineering*. 2023; 53:103582.
6. Richard I. Foster, James TM. Amphlett, Kwang-Wook Kim, Timothy Kerry, Keunyoug Lee, Clint A. Sharrad. Sohio process legacy waste treatment: uranium recovery using ion exchange. *J.Ind.Eng. Chem*. 2020; 81:144-152.
7. Michael Hoyer, Denise Zabelt, Robin Steudtner, Vinzenz Brendler, Roland Haseneder, Jens-Uwe Repke. Influence of speciation during membrane treatment of uranium-contaminated water. *Separation and Purification Technology*. 2014; 132: 413-421.
8. Barkat MA. New trends in removing heavy metals from industrial wastewater. *Arabian Journal of Chemistry*. 2011; 4: 361-377.
9. Nibou D, Khemaissia S, Amokrane S, Barkat M, Chegrouche S, Mellah A. Removal of UO_2^{2+} onto synthetic NaA zeolite. Characterization, equilibrium and kinetic studies. *Chemical Engineering Journal*. 2011; 172:296– 305.
10. Shamshad Khan, Raheel Anjum, Muhammad Bilal. Revealing chemical speciation behaviours in aqueous solutions for uranium (VI) and europium (III) adsorption on zeolite. *Environmental Technology & Innovation.* 2021; 22:101503
11. Jneziménez-Reyes M, Almazan-Sanchez PT, Solache-Ríos M. Radioactive waste treatments by using zeolites. A short review. *Journal of Environmental Radioactivity*.2021; 233:106610.
12. Liu X, Tian R, Ding W, He Y, Li H. Adsorption selectivity of heavy metals by Na-clinoptilolite in aqueous solutions. *Adsorption.* 2019; 25: 747–755.
13. Eduardo Pérez-Botella, Susana Valencia, and Fernando Rey. Zeolites in Adsorption Processes: State of the Art and Future Prospects. *Chem. Rev*. 2022; 122; 17647−1769.
14. Xiu Bai, Jin Zhang, Chong Liu, Shtao Xu, Yingxu Wei, Zhongmin Liu. Solid-state NMR study on dealumination mechanism of H-MOR zeolite by high-temperature hydrothermal treatment. *Microporous and Mesoporous Materials*. 2023, 354:112555
15. Daniele S. Oliveira, Rafael B. Lima, Sibele B. C. Pergher, Vinicius P. S. Caldeira. Hierarchical Zeolite Synthesis by Alkaline Treatment : Advantages and Applications. *Catalysts*. 2023; 13; 316 :1-28
16. Javier Pérez-Ramirez, Claus H. Christensen, Kresten Egeblad, Christina H Christensen, Johan C. Groen, Hierarchical zeolites: enhanced utilisation of microporous crystals in catalysis by advances in materials design. *Chemical Society Reviews*. 2008; 37:2530–2542.
17. Egeblad K, Christensen CH, Kustova M, Christensen CH. Templating mesoporous zeolites. *Chem. Mater*. 2008; 20: 946–960.
18. Khemaissia S. Synthesis and characterization of zeolite-type materials and their applications in the treatment of radioactive waste.USTHB Doctoral Thesis, 2008.
19. Barbara Gil, Lukasz Mokrzycki, Bogdan Sulikowski, Zbigniew Oleijniczak, Stanislaw Walas. Desilication of ZSM-5 and ZSM-12 zeolites: Impact on textural, acidic and catalytic properties. *Catalysis Today*. 2010; 152: 24-32.
20. Xiao Yu Guo, Yan Zeng, Rungtiwa Kosol, Xinhua Gao, Yoshiharu Yoneyama, Guohui Yang, Noritatsu Tsubaki, Catalytic oligomerisation of isobutyl alcohol to jet fuels over dealuminated zeolite Beta. *Catalysis Today*. 2021; 368: 196-203
21. J. Fritz, J. M. Johson-Richard. Colourimetric uranium determination with Arsenazo. *Analytica Chimica Acta*. 1959; 20:164-171.
22. Savvin SB. Analytical Applications of Arsenazo III. Part II: determination of thorium, uranium, protactinium, neptunium, hafnium and scandium. *Talanta*. 1964;11: 1-6.
23. Chloé Bertrand-Drira. Optimization of the texture of zeolite catalysts for the oligomerization of olefins. Doctoral thesis, Ballard School of Chemical Sciences, France, 2014.
24. Farzad Jokar, Seyed Mehdi Alavi, Mehran Rezaei. Investigating the hydroisomerization of n-pentane using Pt supported on ZSM-5, desilicated ZSM-5, and modified ZSM-5/MCM-41. *Fuel*. 2022; 324:124511
25. Loiola AR, Andrade JCRA, Sasaki JM, Silva LRD. Structural analysis of zeolite NaA synthesized by a cost-effective hydrothermal method using kaolin and its use as a water softener. *Journal of Colloid and Interface Science*. 2012; 367; 1: 34-

39.
26. Hirohisa Yamada, Shingo Yokoyama, Yujiro Watanabe, Hikaru Uno, Kenji Tamura.Micro-cubic glass from pseudomorphism after thermal treatment of ammonium-exchanged zeolite A. *Science and Technology of Advanced Materials*. 2005; *6* : 394–398
27. Olson DH, Haag WO, Borghard WS. Use of water as a probe of zeolitic properties: interaction of water with HZSM-5. *Microporous and Mesoporous Materials*.2000; 36: 435-446.
28. Stelzer J, Paulus M, Hunger M., Weitkamp J. Hydrophobic properties of all-silica zeolite beta.*Microporous and Mesoporous.*1998; 22,1-3: 1-8.
29. Kubů M, Žilková N, & Čejka J.Post-synthesis modification of TUN zeolite: Textural, acidic and catalytic properties. *Catalysis Today*.2011; 168: 63-70.
30. Kim Y, Kim YK, Kim JH, Yim MS, Harbottle D, & Lee JW.. Synthesis of functionalized porous montmorillonite via solid–state NaOH treatment for efficient removal of cesium and strontium ions. *Applied Surface Science.* 2018; 450: 404-412.
31. Monama W, Mohiuddin E, Thangaraj B, Mdleleni MM, & Key D. Oligomerization of lomwer olefins to fuel range hydrocarbons over texturally enhaced ZSM-5 catalyst. *Catalysis Today*.2020; 342:167-177
32. Zhu J, Liu Q, Li Z, Liu J, Zhang H, Li R, & Wang J. Efficient extraction of uranium from aqueous solution using an amino-functionalized magnetic titanate nanotubes. *Journal of Hazardous Materials*. 2018; 353: 9–17.
33. Donat R. The removal of uranium (VI) from aqueous solutions onto natural sepiolite. *J. Chem, Thermodynamics*. 2009; 41: 829-835.
34. Saeed Abbasizadeh, Ali Reza Keshtkar, Mohammad Ali Mousavian. Preparation of a novel electrospun polyvinyl alcohol/titanium oxide nanofiber adsorbent modified with mercapto groups for uranium(VI) and thorium(IV) removal from aqueous solution. *Chemical Engineering Journal*. 2013; 220: 161–171
35. Han R, Zou W, Wang Y, Zhu. Removal of uranium (VI) from aqueous solutions by manganese oxide coated zeolite: discussion of adsorption isotherms and pH effect. *Journal of Environmental Radioactivity*. 2007; 93: 127-143.
36. Abbasizadeh S, Keshtkar A. R, Mousavian M. A. Preparation of a novel electrospun polyvinyl alcohol/titanium oxide nanofiber adsorbent modified with mercapto groups for uranium (VI) and thorium (IV) removal from aqueous solution. *Chemical Engineering Journal.*2013; 220: 161-171.
37. Li Y, Wang Y, Li Z, Liu Q, Liu J, Liu L, Zhang X, Yu J, Ultrasound-assisted synthesis of Ca-Al hydrotalcite for U(VI) and Cr(VI) adsorption. *Chemical Engineering Journal*.2013; 218: 295-302.
38. Khemaissia S, Benturki A, Bendjeriou F, Benyounes H, Berrached A. Treatment of uranium effluents by adsorption process on the KLTL zeolite material: Kinetic, thermodynamic and isothermal study of adsorption. *Algerian J. Env. Sc. Technology.*2017; 3(1): 15-28.
39. Langmuir I. The adsorption of gases on plane surfaces of glass, mica and platinum. *Journal of the American Chemical Society*. 1918; 40: 1361-1403.
40. Freundlich H. Over the adsorption in solution. *Journal. Physics Chemistry.*1906; 57:384-470.
41. Dubinin MM, Radushkevich LV. *Chemisches Zentralblatt.*1947;1: 875-890.
42. Zhao D, Wang X, Yang S, Guo Z, Sheng G. Impact of water quality parameters on the sorption of U(VI) onto hematite. *Journal of Environmental Radioactivity* .2012; 103: 20-29.
43. Ho Y.S., MCKAY, G. Pseudo-second order model for sorption process. *Biochem.* 1999; 34: 451-465.
44. Fasfous I, Dawoud J N. Uranium (VI) sorption by multiwalled carbon nanotubes from aqueous solution. *Applied Surface Science*. 2012; 259: 433-440.
45. HO, YS. Citation review of Lagergren Kinetic rate equation on adsorption reactions. *Scientometrics.*2004; 171-177.
46. Amir A. Elzoghby, Ahmed Bakry, Ahmed M. Masoud, Wael S, Mohamed Mohamed H. Taha FH. Synthesis of polyamide-based nanocomposites using green-synthesized chromium and copper oxide nanoparticles for the sorption of uranium from aqueous solution. *Journal of Environmental Chemical Engineering.* 2021; 9: 106755 202.

Recommended Citation

Oudjer F, Khemaissia S, Mouhelbi L, Outtas S,Hammache Y, Meddour Y, Chouial H. Effects of desilication and dealumination of NaA zeolite on uranium recovery from aqueous effluents. *Alger. J. Eng. Technol. 2023*, 8(2), 277-287. https:/dx.doi.org/10.57056/ajet.v8i2.134